

# LASER BEAT-WAVE MICROBUNCHING OF RELATIVISTIC ELECTRON BEAM IN THE THZ RANGE

S. Ya. Tochitsky, S. Reiche, C. Sung,  
J. B. Rosenzweig, C. Pellegrini, and C. Joshi

Neptune Laboratory, Departments of Electrical Engineering and Physics, University of California,  
Los Angeles, CA 90095, USA.

## Abstract

Laser-driven plasma accelerators have recently demonstrated a  $\sim 1$  GeV energy gain of self-trapped electrons in a several-centimeter-long plasma channel. Potential staging of such devices will require the external injection of an electron beam prebunched on the scale of 1-10 THz into a plasma accelerating structure or plasma LINAC. Seeded FEL/IFEL techniques can be used for modulation of the electron beam longitudinally on the radiation wavelength scale. However, a seed source in this spectral range is not available. At the UCLA Neptune Laboratory a Laser Beat-Wave (LBW) microbunching experiment has begun. The interaction of the electron beam and the LBW results in ponderomotive acceleration and energy modulation on the THz scale. This stage is followed by a ballistic drift of the electrons, where the gained energy modulation is transferred to the beam current modulation. Then the beam is sent into a 33-cm long undulator, where a coherent start-up of THz radiation takes place, and the THz pulse is used for a bunching analysis. The performance of LBW bunching is simulated and analyzed using a 3D FEL code for the parameters of an existing photoinjector and two-wavelength TW CO<sub>2</sub> laser system.

## INTRODUCTION

Recently, experiments on laser-driven plasma accelerators have shown acceleration gradients much higher than those of conventional accelerators in a short distance [1] and energy gain around 1 GeV in a several-centimeter-long plasma channel. In spite of the demonstrated high gradients, the potential of laser-plasma accelerators for the next generation of particle accelerators cannot be ascertained without solving the issue of matching a particle beam to the plasma accelerating structure and the efficient extraction of this beam from such a structure. This is important for optimizing the energy extraction efficiency (beam loading) as well as for staging these plasma-based structures. To study these issues a beam of electrons bunched on a scale shorter than the wavelength of the accelerating structure and with the same periodicity has to be injected into a plasma accelerator or a plasma LINAC. For a plasma wave resonantly driven at plasma densities  $10^{16}$ - $10^{18}$  cm<sup>-3</sup>, the plasma wavelength is equal to  $\sim 340$ - $30$   $\mu$ m (1-10 THz), respectively. In order to inject electrons into a narrow phase interval of the plasma wave, an electron beam needs to be prebunched into a series of

$\sim 50$ - $15$   $\mu$ m long microbunches that are separated by the terahertz plasma wavelength.

A seeded inverse free electron laser technique can be used to produce a train of microbunches modulated at a wavelength around  $10$   $\mu$ m [2]. However, a high-power seed source is not available in the THz radiation range.

As was shown theoretically, a high-power Laser Beat-Wave (LBW) modulates the axial momentum of a copropagating relativistic electron beam [3]. The interaction between the electron beam and the LBW in vacuum modulates the electron momentum at the frequency of the beat envelope associated with interference of the two laser lines and can be easily tuned to the THz spectral range. The goal of an LBW microbunching experiment at the UCLA Neptune Laboratory is to study ponderomotive acceleration and energy modulation of a relativistic electron beam on the THz scale.

In this paper, we report the design of the THz microbunching experiment. The performance of LBW bunching is simulated and analyzed using the 3D FEL code Genesis 1.3.

## THZ MICROBUNCHING EXPERIMENT AT THE NEPTUNE LABORATORY

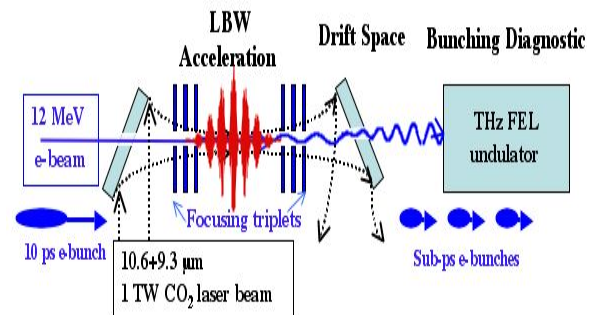


Figure 1: Schematic of LBW THz microbunching experiment at Neptune Laboratory.

The Neptune Laboratory at UCLA hosts a TW class CO<sub>2</sub> laser, providing a natural comb of lines with the LBW in the range of 1-5 THz, and a 12 MeV photoinjector synchronized with the CO<sub>2</sub> laser [4]. A scheme of the LBW microbunching experiment is shown in Fig. 1. Here the two-wavelength CO<sub>2</sub> laser beam with a peak power of around 1 TW (200 J, 200 ps) is focused into the vacuum chamber using an F/15 parabolic mirror. At the focal point the laser beam size  $w_0$  at  $1/e^2$  level is

~180  $\mu\text{m}$  providing an intensity of  $4 \times 10^{14}$  W/cm<sup>2</sup>. For the experiment we consider the LBW between the 10.6 and 9.6  $\mu\text{m}$  lines ( $\lambda_{\text{LBW}} \approx 100$   $\mu\text{m}$ ) as well as the 10.6 and 9.3  $\mu\text{m}$  lines ( $\lambda_{\text{LBW}} \approx 77$   $\mu\text{m}$ ). A 10-ps full width at half maximum electron bunch produced by an RF photoinjector is injected in the LBW. A 12 MeV electron beam with an energy spread of 0.5% is focused down to 200  $\mu\text{m}$  ( $\sigma_{\text{rms}}$ ) at the laser focal plane. We anticipate that bunches with a charge well in excess of 0.5 nC will be produced, providing a peak current of 60 A.

The interaction of the electron beam and the LBW results in ponderomotive acceleration and energy modulation of particles on the THz scale. This stage is followed by a ballistic drift of the electrons over approximately a 1.5 m long distance, where the gained energy modulation transfers to the beam current modulation and, therefore, THz bunching. The CO<sub>2</sub> laser beam is transported out of the vacuum after the laser fluence falls down to the safe level and could be recycled. A quadrupole triplet installed here matches the beam envelope to the natural focusing of a short undulator. The 33-cm long undulator magnet with a period of 3.3 cm and a K value of 1.8 is designed to be resonant to the LBW wavelength. A coherent start-up of THz generation takes place in the undulator owing to the current modulation. The undulator works as a single-shot diagnostic of a bunched electron beam, since the power of THz undulator radiation is directly related to the amplitude of current modulation of the injected electrons. Thus, analysis of both the THz undulator radiation and the coherent transition radiation, measured by a Golay cell, is considered to be the main diagnostic for ponderomotive LBW microbunching.

An alternative view on the LBW microbunching scheme in Fig. 1 is one of an optical klystron where the energy modulated electron beam coming out of the LBW is seeded in a THz FEL producing a high-power radiation pulse. Although the direct injection of LBW into the THz undulator will uncover a new mechanism for seeding FELs, it requires a relatively long (~2 m) undulator [5]. In the case of successful implementation of the described LBW experiment with a short undulator, in the future we consider seeding the 2-m long FEL undulator with a LBW and producing THz pulses of MW power.

## RESULTS OF MODELING OF THE LBW MICROBUNCHING EXPERIMENT

To study the interaction of an electron beam with a LBW and the resonant emission within a periodic magnetic field of an undulator, an analytical model for the interaction was derived and included in the FEL code Genesis 1.3. The underlying model is based on the model and numerical results by D. Gordon et al. [3]. The electric field of the linear polarized fundamental Gaussian beam with the transverse component  $E_x$  and the longitudinal component  $E_z$  is given by

$$E_x = E_0 \frac{w_0}{w} \exp\left(-\frac{r^2}{w^2}\right) \cos\phi$$

and

$$E_z = 2E_0 \frac{w_0}{w} \frac{x}{kw^2} \exp\left(-\frac{r^2}{w^2}\right) \left(\sin\phi - \frac{z}{z_0} \cos\phi\right)$$

where  $x$  is the transverse position with respect to the laser axis,  $z$  is the longitudinal position with respect to the waist position,  $z_0$  is the Rayleigh length,  $k$  is the wavenumber,  $w_0$  the spot size at the best focus and  $w(z) = w_0 \sqrt{1 + (z/z_0)^2}$  is the spot size at a given  $z$ ,  $E_0$  is the field amplitude and the phase at the laser frequency is given by

$$\phi_{0,1} = k_{0,1}z - \omega_{0,1}t + \frac{r^2}{w^2} \frac{z}{z_0} - \tan^{-1}\left(\frac{z}{z_0}\right).$$

The difference between the two frequencies is apparent only in the radiation phase and it is indicated by the indices 0 and 1, respectively.

The beatwave has two characteristic phases, corresponding to the sum and difference of the phases of the individual modes:

$$\phi = \frac{1}{2}(\phi_1 + \phi_2) = \tilde{k}z - \tilde{\omega}t + \frac{r^2}{w^2} \frac{z}{z_0} - \tan^{-1}\left(\frac{z}{z_0}\right)$$

and  $\Phi = Kz - \Omega t$  with  $\tilde{k}$  and  $\tilde{\omega}$  as the mean values of the wavenumbers and frequencies and  $K = (k_0 - k_1)/2$  as well as  $\Omega = (\omega_0 - \omega_1)/2$ . In the modeling process two fundamental Gaussian beams with different frequencies but the same waist position, size and Rayleigh length are overlaid, forming a beat wave. It can easily be shown that the strong transverse electric field excites a transverse oscillation. As a result the electrons on axis will be pushed to an off-axis position and, therefore, start experiencing a non-vanishing longitudinal accelerating field  $E_z$ . The transverse position of the electron can be very well approximated from  $x = (2\gamma/k)a(z)\cos\phi$ , where  $a(z)$  is the slowly varying part of the normalized vector potential of the laser field given by  $a(z) = [(eE_0/kmc^2)(w_0/w)\cos\phi]$ .

If the two frequencies lie close together many wavelengths of the sum-mode as well as the optical laser field slip over an electron while it propagates through the waist of the Gaussian beam. The net impact on the electron is averaged out to zero after it leaves the  $2z_0$  region. On the other hand, the slippage of the difference mode or the LBW can be comparable to the Rayleigh length owing to its slower phase velocity. This makes possible acceleration of some electrons and deceleration of others on the scale of the LBW and results in an energy modulation controlled by the nonlinear ponderomotive force.

The change in the electron energy is incorporated in the code using the analytical expression for energy modulation as

$$\frac{d\gamma}{dz} = \frac{z}{z_0^2} \frac{\gamma a(z)^2}{1 + (z/z_0)^2} \cos^2\Phi.$$

The interaction phase  $\Phi$  is integrated piece-wise with an integration step length much shorter than the Rayleigh length. All fast oscillating terms, which are proportional to  $\sin\phi$  and  $\cos\phi$ , are omitted in the calculation.

Modeling was carried out for the experimental arrangement presented in Fig. 1 with the actual drift distances and the position of focusing magnets in the Neptune Laboratory. The rather pessimistic values of 10 keV for the intrinsic energy spread and 16 mmxrad for the emittance were taken for the electron beam. The dynamics of the growth in the current modulation and radiation power is presented in Fig.2. This case has a perfect overlap of the electron beam waist position with the laser beam containing 500 GW per CO<sub>2</sub> laser line and the LBW at 77  $\mu$ m.

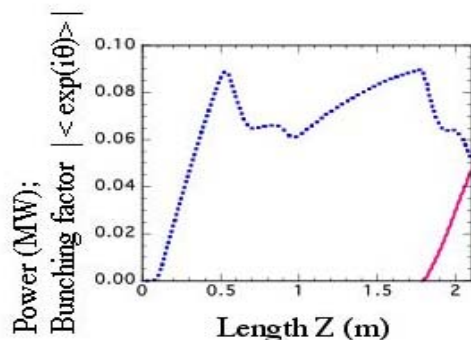


Figure 2: The current modulation (dotted line) and the THz power at 77  $\mu$ m (solid line) along the Neptune beam line.

After the LBW interaction at  $z=9$  cm the current modulation grows almost linearly before the beam enters the focusing quadrupole triplet, the first magnet of which is located at  $z=36$  cm. This focusing triplet is necessary to preserve the beam size until the diverging laser beam is possible to decouple from the particle beam at  $z=140$  cm. The dispersion within the triplet slightly decreases the current modulation, however, after the quads the modulation continues to grow bringing the bunching factor to 9% at the undulator entrance plane ( $z=170$  cm). The bunching factor  $F = |\langle \exp(i\theta) \rangle|$ , where  $\theta$  is the phase at which each electron is located inside the period of a THz wave, is proportional to the ratio of the bunch length and the separation between bunches. As seen in Fig.2, inside the undulator the  $F$  value decreases due to the fact that the electron beam modulation after the long drift is not linear any more or the electron beam is overbunched. At the same time the THz FEL radiation reaches almost 50 kW of power at 77  $\mu$ m, that is two orders of magnitude above the detection threshold of the Golay cell. Note that simulations indicate that the level of SASE emission for the 33-cm long magnet is more than  $10^5$  times smaller than the seeded undulator radiation. This makes the measurement of the THz radiation a convenient diagnostic tool to study microbunching in the single shot experiment.

Due to the availability of the 33-cm long undulator with fixed parameters, we looked at the resonant energy of the

electron beam to yield the maximum power at 77  $\mu$ m. As seen in Fig.3a, the resonance is observed at  $\gamma=24.5$ , where the radiation power is reaching 60 kW.

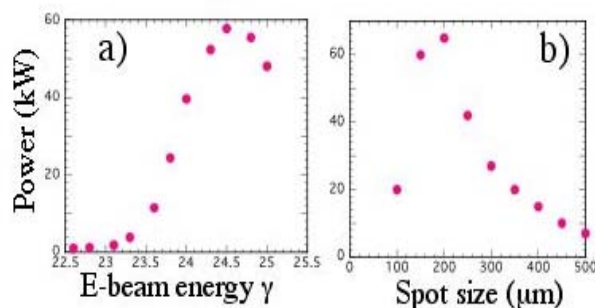


Figure 3: THz power at 77  $\mu$ m as a function of energy of the electron beam (a) and the laser spot size (b).

Fig. 3b shows the results of the THz power optimization for different laser focal spot sizes when the electron beam size is 200  $\mu$ m ( $\sigma_{rms}$ ) and the total laser power is fixed. The maximum is achieved when the laser beam is smaller than the electron beam size. In this case the on-axis electrons see a higher laser field and being modulated more strongly emit coherently in the undulator. However, for a more uniform energy modulation of all electrons, it may be desirable to have the laser beam waist that is larger than the electron beam size. This would be a favorable mode of operation for the LBW microbunching and needs to be studied.

## STATUS AND FUTURE PLANS

In this paper, we describe the LBW microbunching based on the interaction of the nonlinear ponderomotive force of a high-power laser field with the relativistic electron beam in vacuum. The simulations have shown that for parameters achievable at the Neptune laboratory it is possible to study this novel mechanism of microbunching on the THz scale. We plan to run this experiment later this year.

Work supported by the U.S. Department of Energy under Contract No. DE-FG03-92ER40727.

## REFERENCES

- [1] J. Faure, Y. Glinec, A. Puhov et al, Nature., vol. 431, pp. 541-544 (2004).
- [2] W. D. Kimura, M. Babzien, I. Ben-Zvi, et al, Phys. Rev. Lett., vol. 92, 054801-1-054801-4 (2003).
- [3] D. Gordon, C.E. Clayton, T. Katsouleas et al, Phys. Rev. E, vol. 57, pp.1035-1041 (1998).
- [4] S. Ya. Tochitsky, C.E. Clayton, K.A. Marsh, et al, AAC Proceeding 2004, pp. 663-669.
- [5] S. Reiche, C. Joshi, C. Pellegrini et al. NIMP A, to be published (2006).